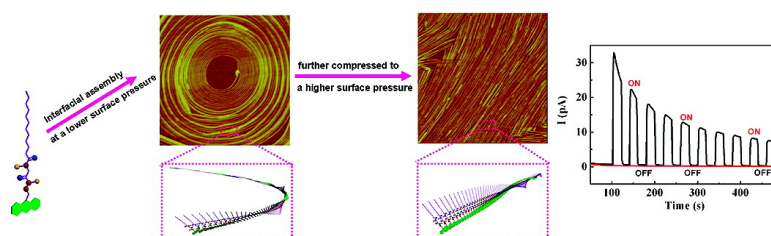Communication

Controllable Fabrication of Supramolecular Nanocoils and Nanoribbons and Their Morphology-Dependent Photoswitching

Yiqun Zhang, Penglei Chen, Lang Jiang, Wenping Hu, and Minghua Liu

More About This Article

Additional resources and features associated with this article are available within the HTML version:

- Supporting Information
- Access to high resolution figures
- Links to articles and content related to this article
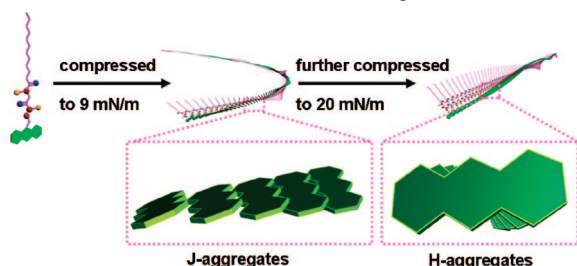- Copyright permission to reproduce figures and/or text from this article

View the Full Text HTML

Controllable Fabrication of Supramolecular Nanocoils and Nanoribbons and Their Morphology-Dependent Photoswitching

Yiqun Zhang, Penglei Chen,* Lang Jiang, Wenping Hu,* and Minghua Liu*

Beijing National Laboratory for Molecular Science, Institute of Chemistry, Chinese Academy of Sciences, P. R. China, 100190

Received July 28, 2008; E-mail: chenpl@iccas.ac.cn; huwp@iccas.ac.cn; liumh@iccas.ac.cn

Recently, nanomaterials with unique morphologies have received great attention owing to their fascinating morphology-dependent properties.[1,2] Such morphologically dependent properties play an important role in designing nanodevices. Therefore, several inorganic or hybrid organic−inorganic nanosystems have been investigated,[1,2] whereas examples based on organic nanomaterials are fewer.[3] In contrast to inorganic nanomaterials, organic nanosystems have peculiar electronic and optical properties and can render considerable variety and flexibility in the molecular design and tunability of physicochemical properties, which make them promising candidates for nanodevices.[4] Thus, investigation on the morphology-dependent properties of organic nanosystems should be an important topic to be explored intensively.

We herein report a controllable fabrication of supramolecular nanocoils and straight nanoribbons of an anthracene derivative, *N*-(2-(2-(9-anthrylmethylene)hydrazino)-2-oxoethyl)dodecan-amide (AN, Figure 1), and their morphologically dependent photoswitching. We

Figure 1. $\pi−A$ isotherm of AN (A). AFM images of the films deposited at (B, C) 9 and (D, E) 20 mN/m. Bottom left corner: molecular structure of AN. The substrates are single face polished silicon wafers (Si(111)).

find when the Langmuir film of AN at the air/water interface is compressed to different surface pressures, nanostructures with different morphologies can be obtained in the deposited Langmuir−Blodgett (LB) films. Nanocoils are formed at a lower surface pressure, whereas the coiled structures can be transformed to straight nanoribbons when the surface pressure increases. Interestingly, the LB films can be built into two-end devices, and a morphology-dependent photoswitching property has been realized. Our investigation suggests that the interfacial organization of organic building blocks might provide a facile way to control the morphologies as well as the corresponding properties of the ultrathin films.

A plateau region and an inflection point are observed from the surface pressure−molecular area ($\pi−A$) isotherm of AN (Figure 1), indicating that the molecular packing might be surface pressure dependent. We deposited the LB films at 9 and 20 mN/m, which were before and after the plateau region, respectively. Nanocoils, which consists of curved nanoribbons, are observed from the AFM

images of the films deposited before the plateau region (9 mN/m, Figure 1B, C). The diameter of the nanocoil ranges from ca. 500 nm to ca. 2 μm. The nanoribbons are ca. 3.5 nm in height, 50−100 nm in width, and several hundred micrometers in length. For the LB films transferred after the plateau region (20 mN/m, Figure 1D, E), its morphology is exhibited as straight nanoribbons.

The nanostructures were deposited on octadecyltrichlorosilane modified quartz substrates by an LB technique. Au electrodes were thermally evaporated using a micrometer-sized Au wire as the mask to obtain gap electrodes (gap width: ca. 20 μm). The photoswitching characteristics of thus fabricated two-end devices are presented in Figure 2A. The LB film transferred at 20 mN/m shows a photoswitch-

Figure 2. (A) Photoswitching characteristics of the two-end devices based on the films of AN by white light; the electrodes are Au, the gap width is 20 μm, and the power of illumination is 5.76 mW/cm^2 at bias 50 V. (B) UV−vis spectra of AN in acetonitrile solution (black) and in the films deposited at (red) 9 and (green) 20 mN/m. The substrates are quartz slides.

ing property during the on/off process, whereas the film transferred at 9 mN/m displays a negligible photocurrent response. For the film deposited at 20 mN/m, the corresponding device display a switching ratio around 43−28. With the shortening of the gap width, the switching ratio increased (Figures S1, S2). This is probably because the shorter conducting channel is more efficient for the transport and collection of photogenerated free carriers. The photocurrent shows a decreasing tendency, which is similar to the photocurrent response properties of the LB films of other systems.[5] Our results show that a morphology-dependent photoswitching can be realized in the supramolecular films.

Anthracene derivatives are excellent organic semiconductors whose carrier mobility is, to a great extent, determined by π-stacking crystal packing.[6] The π-stacking status of our nanocoil and straight nanoribbon were characterized by UV−vis and CD spectra. The UV−vis spectrum of AN in acetonitrile solution exhibits an intense ^1B_b absorption at 255 nm (Figure 2B). A typical anthracene absorption in the region 310−450 nm, centering at 388 nm and ascribing to the ^1L_a band, is also observed.[7] A ^1B_b band maximum at 257 nm, red-shifted by 2 nm compared with that in solution, is observed from the film deposited at 9 mN/m. This indicates the anthracene chromophores are arranged in J-aggregates in the nanocoils. For the film deposited at 20 mN/m, a ^1B_b band at 241 nm, blue-shifted by 14 nm compared with that in solution, is

detected. The ^1B_b band is also accompanied by a shoulder peak centered at 257 nm. These results indicate most of the J-aggregates, formed before the plateau region, are transformed to H-aggregates upon increasing surface pressure. As shown in Scheme 1, slight

Scheme 1. Formation of Nanocoils and Straight Nanoribbons[a]

[a] The alkyl chains take trans-zigzag and gauche conformations in the nanocoil and nanoribbon, respectively, both of which are schemed in a straight conformation for simplicity. The intermolecular hydrogen bonds between amide hydrogens and carbonyl groups are omitted for clarity. An optimized supramolecular assembly is presented in Figure S6.

$\pi-\pi$ overlapping exists in the J-aggregates, whereas relatively strong $\pi-\pi$ overlapping occurs in the H-aggregates.

It should be noted the ^1L_a band, which is maximum at 388 nm in solution, is red-shifted to 395 and 390 nm for the films deposited at 9 and 20 mN/m, respectively. These red shifts can be assigned to the formation of "oblique aggregates", where the dipole moments of the anthracene rings are staggered at a certain angle rather than exactly parallel to each other.[8] This inspired us to investigate the circular dichroism (CD) spectra of the films (Figure S4).[9] The film deposited at 9 mN/m shows no CD signals, while that deposited at 20 mN/m exhibits a Cotton effect with an exciton couplet.[7] This indicates the molecules have experienced symmetry breaking at the air/water interface at a higher surface pressure.[9] The film deposited at 9 mN/m displays no CD signal, indicating the chromophores are not stacked efficiently. However, the strong exciton couplet indicates the neighboring chromophores are stacked in a rather close way in the film deposited at 20 mN/m. These results indicate only a slight $\pi-\pi$ overlapping exists in the film deposited at 9 mN/m, while the $\pi-\pi$ overlapping is large in the film deposited at 20 mN/m, where the anthracene chromophores are arranged as H-aggregates.

Quantum mechanical calculations and structural analysis[10] have predicted that efficient charge transport can be obtained when conjugated molecules have strong interactions with neighboring molecules to maximize the overlap of π molecular orbits. Hence, the larger $\pi-\pi$ overlapping in the film deposited at 20 mN/m is expected to provide more efficient carrier transport. As shown in Scheme 1, the intermolecular hydrogen bonds (FT-IR, Figure S5) together with $\pi-\pi$ interactions link the molecules to form one-dimensional assemblies. Due to the directionality nature of H-bonding, the adjacent units are stacked at a certain angle, resulting in the formation of coiled nanostructures or chiroptical nanoribbons under different surface pressures. When the surface pressure is 9 mN/m, the neighboring anthracene rings show only a slight $\pi-\pi$ overlapping, which disfavors the carrier moving and decreases the carrier mobility μ.[10] When the surface pressure is 20 mN/m, the molecules are compressed to form H-aggregates, resulting in a larger efficient $\pi-\pi$ overlapping. This kind of packing favors the carrier moving and giving an appropriate carrier mobility μ.[9] The different molecular packings in these two types of nanostructures, and their different responses to the photoirradiation, would cause a difference in the number of free carriers and in the carrier mobility, which should be responsible for their different photocurrent response properties.[10] Actually, under photoirradiation, there are two possible working mechanisms for the devices. One is

similar to that of organic photovoltaic devices, but in our case no photovoltage was observed. Another possible mechanism is that the films worked as a photoconductor. When an incident light falls on the surface of the photoconductor, carriers are generated, resulting in an increase of conductivity ($\sigma = ne\mu$, where σ is the conductivity, n is the number of carriers, e is the charge of the electron, and μ is the mobility). The results of Figure 2A demonstrate that the films deposited at 20 mN/m have a very high sensitivity to photoirradiation. It is highly possible that such films work as a photoconductor in this case. From the UV–vis spectra, the energy gap of the AN is estimated to be ca. 2.6 eV. This value is narrow enough to permit the generation of substantial numbers of charge carriers by white light irradiation.[4a]

In summary, we have shown AN could be controllably assembled to nanocoils and straight nanoribbons through the interfacial organization at different surface pressures. While the nanocoils do not show the photocurrent response, the nanoribbons exhibit a photocurrent, which is switchable during the on/off process. The results open up a facile way to fabricate controllable nanostructures showing a morphology-dependent property.

References

(1) (a) El-Sayed, M. A. *Acc. Chem. Res.* **2001**, *34*, 257. (b) Baughman, R. H.; Zakhidov, A. A.; De Heer, W. A. *Science* **2002**, *297*, 787. (c) Larsson, E. M.; Alegret, J.; Käll, M.; Sutherland, D. S. *Nano Lett.* **2007**, *7*, 1256. (d) Bell, D. J.; Bauert, T. E.; Zhang, L.; Dong, L. X.; Sun, Y.; Güutzmacher, D.; Nelson, B. J. *Nanotechnology* **2007**, *18*, 055304.
(2) (a) Li, X.; Zhang, L.; Wang, X.; Shimoyama, I.; Sun, X.; Seo, W.; Dai, H. *J. Am. Chem. Soc.* **2007**, *129*, 4890. (b) Xia, Y.; Yang, P.; Sun, Y.; Wu, Y.; Mayers, B.; Gates, B.; Yin, Y.; Kim, F.; Yan, H. *Adv. Mater.* **2003**, *15*, 353. (c) Patzke, G. R.; Krumeich, F.; Nesper, R. *Angew. Chem., Int. Ed.* **2002**, *41*, 2446. (d) Hurst, S. J.; Payne, E. K.; Qin, L.; Mirkin, C. A. *Angew. Chem., Int. Ed.* **2006**, *45*, 2672.
(3) Reitzel, N.; Hassenkam, T.; Balashev, K.; Jensen, T. R.; Howes, P. B.; Kjaer, K.; Fechtenkötter, A.; Tchebotareva, N.; Ito, S.; Müllen, K.; Björnholm, T. *Chem.—Eur. J.* **2001**, *7*, 4894.
(4) (a) Jiang, L.; Fu, Y.; Li, H.; Hu, W. *J. Am. Chem. Soc.* **2008**, *130*, 3937. (b) Che, Y.; Datar, A.; Balakrishnan, K.; Zang, L. *J. Am. Chem. Soc.* **2007**, *129*, 7234. (c) Balakrishnan, K.; Datar, A.; Naddo, T.; Huang, J.; Oitker, R.; Yen, M.; Zhao, J.; Zang, L. *J. Am. Chem. Soc.* **2006**, *128*, 7390. (d) Tang, M. L.; Reichardt, A. D.; Miyaki, N.; Stoltenberg, R. M.; Bao, Z. *J. Am. Chem. Soc.* **2008**, *130*, 6064. (e) Roberson, L. B.; Kowalik, J.; Tolbert, L. M.; Kloc, C.; Zeis, R.; Chi, X.; Fleming, R.; Wilkins, C. *J. Am. Chem. Soc.* **2005**, *127*, 3069. (f) Zeis, R.; Besnard, C.; Siegrist, T.; Schlockermann, C.; Chi, X.; Kloc, C. *Chem. Mater.* **2006**, *18*, 244.
(5) (a) Lang, A.-D.; Huang, C.-H.; Gan, L.-B.; Zhou, D.; Ashwell, G. J. *Phys. Chem. Chem. Phys.* **1999**, *1*, 2487. (b) Lu, Y.; Spitler, M. T.; Parkinson, B. A. *Langmuir* **2007**, *23*, 11637.
(6) (a) Meng, H.; Sun, F.; Goldfinger, M. B.; Gao, F.; Londono, D. J.; Marshal, W. J.; Blackman, G. S.; Dobbs, K. D.; Keys, D. E. *J. Am. Chem. Soc.* **2006**, *128*, 9304. (b) Zareie, M. H.; Ma, H.; Reed, B. W.; Jen, A. K.-Y.; Sarikaya, M. *Nano Lett.* **2003**, *3*, 139. (c) Meng, H.; Sun, F.; Goldfinger, M. B.; Jaycox, G. D.; Li, Z.; Marshall, W. J.; Blackman, G. S. *J. Am. Chem. Soc.* **2005**, *127*, 2406.
(7) (a) Harada, N.; Nakanishi, K. *Circular Dichroic Spectroscopy-Exciton Coupling in Organic Stereochemistry*; University Science Books: Mill Valley, CA, 1983. (b) Durfee, W. S.; Storck, W.; Willig, F.; von Frieling, M. *J. Am. Chem. Soc.* **1987**, *109*, 1297.
(8) Dutta, A. K. *Langmuir* **1997**, *13*, 5678.
(9) (a) Yuan, J.; Liu, M. *J. Am. Chem. Soc.* **2003**, *125*, 5051. (b) Huang, X.; Li, C.; Jiang, S.; Wang, X.; Zhang, B.; Liu, M. *J. Am. Chem. Soc.* **2004**, *126*, 1322. (c) Qiu, Y.; Chen, P.; Liu, M. *Langmuir* **2008**, *24*, 7200.
(10) (a) Coropceanu, V.; Cornil, J.; da Silva Filho, D. A.; Olivier, Y.; Silbey, R.; Brédas, J. *Chem. Rev.* **2007**, *107*, 926. (b) Mas-Torrent, M.; Hadley, P.; Bromley, S. T.; Ribas, X.; Tarrés, J.; Mas, M.; Molins, E.; Veciana, J.; Rovira, C. *J. Am. Chem. Soc.* **2004**, *126*, 8546. (c) Curtis, M. D.; Cao, J.; Kampf, J. W. *J. Am. Chem. Soc.* **2004**, *126*, 4318.

JA805891K